Liquid Crystals
Publication details, including instructions for authors and subscription information:
http://www.informaworld.com/smpp/title~content=t713926090

Two-dimensional Raman study of the submolecular, electric field-induced reorientation of a nematic liquid crystal

Kelly Huang

Online publication date: 06 August 2010

To cite this Article Huang, Kelly(1998) 'Two-dimensional Raman study of the submolecular, electric field-induced reorientation of a nematic liquid crystal', Liquid Crystals, 25: 6, 745 — 755
To link to this Article: DOI: 10.1080/026782998205769
URL: http://dx.doi.org/10.1080/026782998205769

LIQUID CRYSTALS, 1998, VOL. 25, NO. 6, 745–755

Two-dimensional Raman study of the submolecular, electric field-induced reorientation of a nematic liquid crystal

KELLY HUANG and GERALD G. FULLER*
Department of Chemical Engineering, Standford University, Stanford, CA 94305-5025, USA

(*Received 8 February 1996; accepted 17 July 1998*)

Two-dimensional Raman scattering is presented as a technique for the monitoring of electric field-induced, submolecular reorientation in liquid crystals. The motions of the flexible part and the rigid core of 4-pentyl-(4-cyanophenyl)cyclohexane (PCH5) are independently monitored in response to both step and oscillatory electric fields. Step voltage experiments show that the flexible group reorients before the rigid core. Also, oscillatory electric field experiments demonstrate that the flexible and rigid groups reorient asynchronously. In fact, at periodicities that are shorter than the bulk reorientation times, it is observed that the reorientation of the flexible part is amplified, while the motion of the rigid core is inhibited. The data suggest that the flexible group possesses a small, local dielectric anisotropy that can couple with the electric field to induce an independent, cooperative reorientation when the mobility of the rigid core is restricted.

1. Introduction

Liquid crystals are highly ordered materials, and their ability to rapidly change orientation in the presence of electric fields provides the basis for many applications such as filters, waveguides, and display devices [1, 2]. For this reason, the electro-optical effects in liquid crystals have been extensively studied. Standard techniques for electro-optic characterization, such as measurement of birefringence and dichroism, have been applied to monitor bulk director reorientation in these systems [3]. In these studies, continuum theory has been shown to model effectively the macroscopic orientational coupling to external fields [1, 2]. However, the molecular mechanism by which liquid crystal molecules reorient is not well understood. With the development of time-resolved spectroscopy there have been many recent investigations into the submolecular motions in liquid crystals. These studies suggest that liquid crystal molecules may not reorient as rigid rods and may exhibit submolecular relaxations. A fundamental understanding of these intramolecular motions may lead to the development of better performing liquid crystal systems.

In this paper, a new technique, two-dimensional Raman scattering (2D Raman), is introduced for the study of the microstructural dynamics of a liquid crystal in the presence of an electric field. 2D Raman utilizes the inherent chemical specificity of the Raman effect and has been employed by Huang *et al.* [4] to study microstructural dynamics within the homopolymer polyisobutylene. The technique exploits a new orientation measure, the Raman anisotropy, to monitor the submolecular motions of the liquid crystal with respect to the applied perturbation. Additionally, through two-dimensional correlation analysis of the Raman anisotropy emanating from distinct bond vibrations, the cooperation of the reorientation between different segments of the liquid crystal molecule is investigated.

Specifically, it is observed that the rigid core and flexible part of 4-pentyl-(4-cyanophenyl)cyclohexane (PCH5) exhibit different responses in the presence of an electric field that perturbs the system at time scales that are shorter than the bulk reorientation times. Interestingly, the flexible part reorients before the rigid core even though the dielectric anisotropy is thought to be primarily attributable to the rigid part. Similar observations have been reported by Urano and Hamaguchi [5, 6] for the liquid crystal 4-*n*-pentyl-4′-cyanobiphenyl (5CB). The authors of that study proposed a molecular model that involves the influence of surface molecules to cause a bulk reorientation of the flexible chains [6]. The results for PCH5 presented in this paper indicate that the flexible group actually experiences an electric torque, and surface molecules are not significantly involved in the reorientation of the flexible chains.

Recently, researchers have debated the physical viability of asynchronous motions within liquid crystal molecules. Shilov *et al.* [7] performed Fourier transform infrared spectroscopy (FTIR) on *p*-cyanophenyl *p*-*n*-hexylbenzoate

*Author for correspondence.

0267–8292/98 $12.00

(6CPB) subjected to an electric field. Time domain data after the onset of the electric field and subsequent to cessation indicate that 6CPB reorients as a rigid rod. The authors concluded that the difference in response between moieties is either not general and dependent upon molecular structure or the effect is too small to be detected using time-resolved FTIR. Similar rigid-rod type reorientation has been reported for other liquid crystals [8–10]. De Bleijser *et al.* [11] also used time-resolved FTIR to revisit the electric field-modulated reorientation within 5CB. Frequency domain data showed only synchronous reorientation contrary to observations of Urano and Hamaguchi. De Bleijser *et al.* reason that previously observed differences in intramolecular motions may be due to the possibility that different bands may emphasize different regions of the sample. However, frequency sweep experiments in the present study suggest an additional explanation. Specifically, it is shown that intramolecular reorientation differences occur when the motion of the rigid core is restricted and is, thus, dependent upon the time scale of the perturbing field relative to the bulk reorientation time scale. Discrepancies in experimental observations are reasonable since previous studies have been performed with different liquid crystals, perturbation time scales, temperatures, and sample thicknesses. Frequency sweep experiments, analogous to mechanical experiments monitoring polymer rheology, allow for the probing of liquid crystal response over many orders of time scales. Additionally Raman, as compared with IR spectroscopy, is particularly useful for the study of dynamics over longer time scales with minimal influence of surface molecules since it is not limited to thin samples.

2. Background

2.1. *Two-dimensional Raman scattering*

A comprehensive discussion of 2D Raman has been given elsewhere [4], and a brief discussion of the technique is presented here. The measure of interest is the *Raman anisotropy*, which is related to components of the derived polarizability tensor, α'_{ij}, as follows:

$$\Gamma(\nu) = \langle \alpha'^2_{xx} \rangle - \langle \alpha'^2_{zz} \rangle. \tag{1}$$

Here, x is the preferred orientation direction of the material, light propagates along the y-axis, and the angled brackets refer to an average about the distribution function describing molecular orientation. Archer *et al.* [12] have demonstrated that for a system of rigid rods with the orientation of molecular axes given by unit vectors u_i, the Raman anisotropy is of the form

$$\Gamma(\nu) = \gamma_1(\nu)(\langle u_x^2 \rangle - \langle u_z^2 \rangle) - \gamma_2(\nu)(\langle u_x^4 \rangle - \langle u_z^4 \rangle) \tag{2}$$

where γ_1 and γ_2 are constants particular to vibration ν. Thus, $\Gamma(\nu)$ is linearly related to the difference in the second and fourth moments of the orientational distribution function in the preferred and perpendicular directions within the plane normal to the propagation of light. $\Gamma(\nu) = 0$ for isotropic systems and increases in magnitude monotonically with orientation in the preferred direction. Thus, $\Gamma(\nu)$ can be used to quantify orientation of individual components and submolecular orientation in complex systems using intrinsic bond vibrations as labels.

In addition to characterizing individual component orientation, 2D Raman provides for a measure of interspecies interactions. This is accomplished by cross correlating the dynamic Raman anisotropy arising from distinct constituents. The application of cross correlation analysis to spectroscopic measurements was first proposed by Noda [13, 14] in the development of two-dimensional infrared spectroscopy. In the study presented here, sinusoidal perturbations are utilized to induce orientational changes, but the correlation analysis is applicable to any arbitrary perturbation waveform [15].

The application of a sinusoidal voltage, $V = V^0 \sin(\omega t)$, causes an oscillatory change in the moments of the orientational distribution function, and the Raman anisotropy becomes a dynamic Raman anisotropy, $\tilde{\Gamma}$. Since these nematic liquid crystals reorient equally for positive and negative voltages, $\tilde{\Gamma}$ displays a response at twice the frequency of the applied electric field. Also, since liquid crystals are viscoelastic, the dynamic Raman anisotropy, $\tilde{\Gamma}$, responds out of phase with the field by a phase angle δ and with amplitude Γ^0:

$$\tilde{\Gamma}(\nu) = \Gamma^0(\nu) \sin\{2\omega t + \delta(\nu)\}. \tag{3}$$

Equation (4) shows the limiting cross correlation of $\tilde{\Gamma}$ emanating from the component containing bond vibration ν_1 and the component with bond vibration ν_2:

$$\chi(\tau) = \lim_{\eta \to \infty} \frac{1}{\eta} \int_{\eta/2}^{\eta/2} \tilde{\Gamma}(\nu_1, t)\tilde{\Gamma}(\nu_2, t + \tau)\, \mathrm{d}t \tag{4}$$

where τ is the correlation time. Substitution of equation (3) into equation (4) yields the solution:

$$\chi(\tau) = \Phi(\nu_1, \nu_2) \cos(2\omega\tau) + \Psi(\nu_1, \nu_2) \sin(2\omega\tau). \tag{5}$$

$\Phi(\nu_1, \nu_2)$ is the synchronous correlation intensity:

$$\Phi(\nu_1, \nu_2) = \frac{1}{2}\Gamma^0(\nu_1)\Gamma^0(\nu_2) \cos\{\delta(\nu_1) - \delta(\nu_2)\} \tag{6}$$

and $\Psi(\nu_1, \nu_2)$ is the asynchronous correlation intensity:

$$\Psi(\nu_1, \nu_2) = \frac{1}{2}\Gamma^0(\nu_1)\Gamma^0(\nu_2) \sin\{\delta(\nu_1) - \delta(\nu_2)\}. \tag{7}$$

Since $\Phi(\nu_1, \nu_2)$ is a maximum when $\delta_1 = \delta_2$. It is obvious that large values of the synchronous correlation intensity suggest simultaneous reorientation of the two components. On the other hand, $\Psi(\nu_1, \nu_2)$ is a maximum when the

two species lag the electric field exactly in quadrature with each other. Thus, large values of the asynchronous correlation imply independent reorientation of the two constituents.

2.2. *Splay Fréedericksz transition*

The reorientation of liquid crystals in the presence of an external field is known as a Fréedericksz transition since Fréedericksz *et al.* [16] were the first to observe and study the effects of magnetic fields on liquid crystal orientation. The experimental and theoretical extension to electric fields has been performed by several researchers [17–20]. Electric fields couple with nematic liquid crystals through the dielectric anisotropy, the difference in the dielectric permittivity parallel and perpendicular to the director ($\Delta\varepsilon = \varepsilon_{//} - \varepsilon_{\perp}$). For a liquid crystal with positive dielectric anisotropy, the director tends to align parallel to the field; conversely, molecules with negative dielectric anisotropy align perpendicular to the field. Figure 1 displays the splay Fréedericksz effect that is investigated in this study. As shown, the liquid crystal monodomain is oriented along the x-axis and the application of a electric field, **E**, larger than the threshold field, $\mathbf{E}_{th}$, results in a reorientation of the local directors towards the y-axis. The y-axis is also the propagation direction of the incident and scattered light.

The dynamics of the Fréedericksz transition is expressed as a balance of the elastic, electric, and viscous torques. Pieranski and coworkers [19, 21] developed the dynamic theory for the presence of small magnetic fields that cause slight deviations, characterized by the angle θ, from the initial state. In this limit, the coupling of translational motions with orientational changes can be neglected. Pieranski's solution for the director reorientation in the presence of a step voltage is the following:

$$\theta_m^2(t) = \frac{\theta_m^2(\infty)}{1 + \left[\frac{\theta_m^2(\infty)}{\delta^2} - 1\right] \exp\left\{-\frac{\Delta\varepsilon}{2\pi\gamma_r D^2}(V^2 - V_{th}^2)t\right\}}. \tag{8}$$

Here, $\theta_m(\infty)$ is the steady-state value of the maximum distortion angle found at the centre of the cell, γ_r is the rotational viscosity coefficient, and the threshold voltage is related to $\Delta\varepsilon$ and the splay elastic constant, K, as follows:

$$V_{th} = \pi\left(\frac{4\pi K}{\Delta\varepsilon}\right)^{1/2}. \tag{9}$$

Lastly, $\delta^2 = \langle\theta_m^2(t=0)\rangle$ are the fluctuations in the average director orientation at imposition of the field, and Pieranski [21] demonstrated that δ^2 can be related to the thermal energy $k_B T$ through the following relationship:

$$\delta^2 = \frac{k_B T \log\dfrac{V - V_{th}}{V_{th}}}{\pi K D}. \tag{10}$$

Of more practical interest, equation (8) yields expressions for the response times of the liquid crystal orientation to the application of an electric field. For large times after the onset of the field, equation (8) states that $\theta_m(t)$ approaches $\theta_m(\infty)$ as $\exp(t/\tau_{on})$ with a time constant which is dependent on the magnitude of the external field:

$$\tau_{on} = \frac{4\pi D^2\gamma_r}{\Delta\varepsilon(V^2 - V_{th}^2)} = \frac{4\pi D^2\gamma_r}{\Delta\varepsilon V^2 - 4\pi^3 K}. \tag{11}$$

When the field is turned off, substitution of $V = 0$ into equation (11) yields a relaxation time constant:

$$\tau_{off} = \frac{\gamma_r D^2}{\pi^2 K}. \tag{12}$$

Figure 2 shows equation (8) plotted against time normalized by τ_{on}. There is a slow increase in the

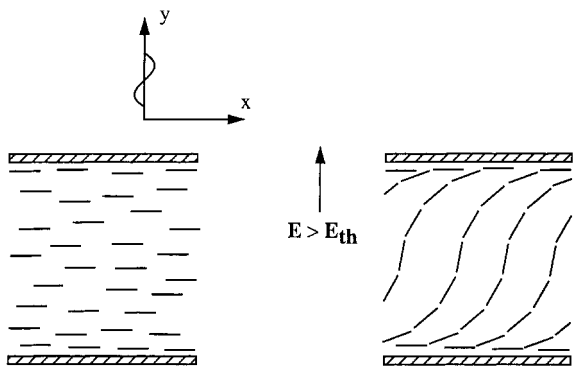

Figure 1. The splay Fréedericksz transition. The left figure shows the initial configuration; the right-figure displays the xy-projection of the director field in the presence of **E**, assuming $\Delta\varepsilon > 0$.

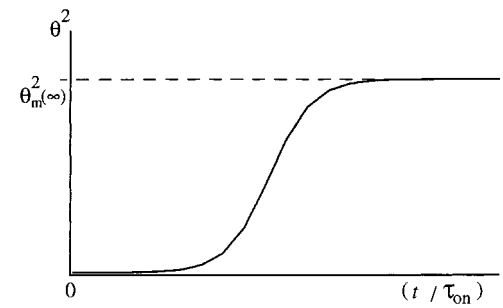

Figure 2. Equation (1) vs dimensionless time.

distortion initially after the field is imposed at time zero and prior to exponential behaviour due to the fact that the initial state is metastable with respect to the perpendicular field. Fluctuations of orientation are necessary to induce the cooperative motion of the molecules to the stable state. In the case of relaxation upon turning off the field, no delay is expected since the system is already in an unstable configuration in the absence of a field. Although equation (11) is solved under the assumption of small θ, it is often used in practice for calculating response times. In fact, equation (11) is valid for larger fields that induce flow if γ_r is replaced by an effective rotational viscosity coefficient, γ_1^* that is dependent on field strength [2, 22]. Pieranski [19] determined that no correction ($\gamma_1^* = \gamma_r$) is necessary for the splay transition induced by voltages approximately $V/V_{th} < 3.25$. On the other hand, for higher voltages $V/V_{th} > 4$, Clark and Leslie [23] demonstrated that the director relaxation at the centre of the cell does not occur monotonically. Rather, under these high voltages, a shear flow is induced that causes further distortion before the eventual relaxation to the planar alignment.

3. Experimental

3.1. *Apparatus*

The 2D Raman optical train, figure 3, is based upon the experimental apparatus developed for polarization-modulated laser Raman scattering [12, 24]. An argon ion laser, operating at 100 mW, provides monochromatic light at 514.5 nm and propagates along the y-axis. The beam is passed through optics to remove plasma lines. These optics consist of an entrance aperture, monochromator grating, mirror, and exit aperture. Then, a polarizer establishes the polarization along the x-axis, and the polarization generating section is completed with a photoelastic modulator (PEM) oriented at 45° to the x-axis. The PEM modulates the polarization of the incident light by introducing a sinusoidal phase retardation at a frequency $f = 10$ kHz in the xz-plane. The transmitted and Raman scattered light from the sample, undergoing flow along the x-axis, are collected with a lens and analysed with a polarizer at 45° to the x-axis. A beam splitter is employed to reflect partially this light to a GaAs photodetector that simultaneously measures birefringence, and a notch filter eliminates the laser line so that the Raman scattered light intensity can be measured using a double monochromator and photomultiplier tube (PMT). In front of the monochromator, a half wave plate is employed to maximize the throughput by offsetting the polarization bias of the gratings.

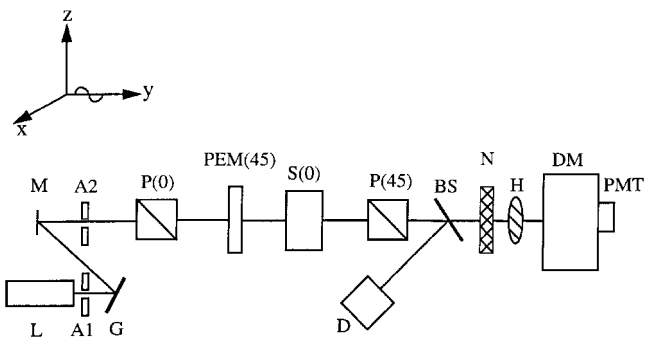

Figure 3. 2D Raman apparatus for simultaneous measurement of the Raman anisotropy and birefringence. The instrument consists of an argon ion laser (L), entrance aperture (A1), monochromator grating (G), mirror (M), exit aperture (A2), linear polarizers (P), photoelastic modulator (PEM), sample (S), beam splitter (BS), notch filter (N), half wave plate (H), double monochromator (DM), photomultiplier tube (PMT), and GaAs detector (D). Light propagates along the y-axis through the sample, which is undergoing oscillatory flow along the x-axis.

3.2. *Signal analysis*

Since the PEM introduces a sinusoidal retardation of the incident light, $\delta_{PEM} = p \sin(ft)$, the signals from the photodetector and PMT are of the form [24].

$$\frac{I}{I_0} = R_{dc} + 2J_1(p)R_f \sin(ft) + 2J_2(p)R_{2f}\cos(2ft) \tag{13}$$

where I_0 is the incident light intensity and $J_1(p)$ and $J_2(p)$ are Bessel function coefficients arising from the Fourier decomposition of the intensity signal. The raw signals are amplified with low-noise current amplifiers and then demodulated using lock-in amplifiers and low-pass filters. For 2D Raman, the component of interest from the Raman scattered intensity measured by the PMT is R_{2f} since it is related to the Raman anisotropy as

$$R_{2f}(\nu) = \frac{1}{4}\tilde{\Gamma}(\nu). \tag{14}$$

Since the Raman anisotropy is a measure of the difference in orientation along the x-axis with respect to the z-axis, the liquid crystal sample aligned along the x-axis is expected to yield a large value for $\Gamma(\nu)$ at equilibrium. Upon the application of a step electric field, it is expected that the magnitude of $\Gamma(\nu)$ will decrease towards zero as the molecules rotate towards the y-axis. For the sinusoidal electric field experiments, $\Gamma(\nu)$ responds at twice the frequency of the field since the liquid crystal response to positive and negative voltages is identical. The R_{dc} component is also acquired for normalization

and is related to the Raman tensor as follows:

$$R_{dc} = \frac{1}{8}\{\langle \alpha'^2_{xx} + \alpha'^2_{zz} + 2\alpha'^2_{zx}\rangle\}. \quad (15)$$

The photodetector, which simultaneously monitor the bulk orientation, provides a measure of the sample's birefringence in the form:

$$R_f^{birf} = \sin(\delta') \quad (16)$$

where δ' is the retardation and is related to the birefringence, $\Delta n'$, by $\delta' = 2\pi\Delta n' d/\lambda$ for light of wavelength λ with path length d.

A computer equipped with an analogue to digital board acquires the signals from the lock-in amplifiers and low-pass filters. The attenuation and roll-off effect of time constants and cut-off frequencies are corrected for using the equations from single pole filter theory [25]. Additionally, for the oscillatory experiments, fast Fourier transforms are utilized to quantify the amplitudes and phases relative to the applied strain, and cross correlation analyses are performed.

3.3. *Sample preparation*

The PCH5 sample used in this study was purchased from EM Industries and used without further purification. PCH5 exhibits a crystal to nematic transition at $T_{CrN} = 30°C$ and a nematic to isotropic transition at $T_{NI} = 55°C$. The liquid crystal material was sandwiched between two indium tin oxide coated slides separated by a teflon spacer. The slides were cleaned in methylene chloride vapour in a reflux container. Subsequently, they were dipped into a 0.5% aqueous solution of poly(vinyl alcohol) ($M_w = 78\,000$) and allowed to air dry. The slides were then unidirectionally rubbed with a velvet cloth to achieve homogeneous alignment. The teflon spacer used was 125 μm thick. A 50 μm spacer was also used to check for depolarization effects on a sample at 30°C. The check showed that there was no thickness effect within the sensitivity of the experiment. As stated by Seeliger *et al.* [26]; PCH5 is less susceptible to depolarization effects than 5CB since PCH5 possesses weaker anisotropic dielectric properties. The monodomain was prepared on a hot stage at approximately 40°C, and the slides were clamped in an aluminium holder. The cell holder was equipped with cartridge heaters and a thermocouple to provide feedback to the temperature controller; the temperature of the cell was regulated within ±0.2°C. After securing the sample within the holder, the cell was heated to the isotropic phase, 60°C, and cooled to the temperature of the experiment. Uniformity in alignment was confirmed by examining the extinction between crossed polarizers and under a polarizing microscope.

4. Results and discussion

The Raman spectrum obtained at 35°C for the 125 μm film of PCH5 is shown in figure 4. The peak regions of interest are readily identifiable through comparison with Raman spectroscopy studies of the similar liquid crystal, 5CB [27]. In order to study the rigid portion of the liquid crystal, this study focuses on the vibrations corresponding to the phenyl CC stretching, ϕ(CC), and the cyano symmetric stretch, ν_s(CN), that appear at 1606 and 2226 cm^{-1}, respectively. The motions of the flexible pentyl chain are monitored using the bonds in the region between 2800 and 2950 cm^{-1}. The CH peaks within this profile region correspond to the methylene symmetric stretch [$\nu_s(CH_2) = 2857\,cm^{-1}$], methyl symmetric stretch [$\nu_s(CH_3) = 2870\,cm^{-1}$], and the methylene anti-symmetric stretch [$\nu_a(CH_2) = 2926\,cm^{-1}$]. It should be noted that the methylene bands may include contributions from the cyclohexane ring along the rigid core; however, such an overlap would not contribute to asynchronous motion with respect to the rigid core since conformation changes in cyclohexane occur on much shorter time scales than those of the experiments.

Since the measure of interest is the Raman anisotropy, figure 5 displays the output from the 2f-lock-in of Γ vs wavenumber for various temperatures. Only highly polarized bands, which are sensitive to macroscopic orientation, give rise to peaks within the Raman anisotropy spectrum. The peaks of interest show a decrease in intensity with increasing temperature within the nematic regime until they sharply vanish above the nematic–isotropic transition temperature. The decrease in Γ is similar to the variation of the order parameters for PCH5 [26]. This is not surprising since the Raman anisotropy is linearly related to the second and fourth moments of the orientational distribution function.

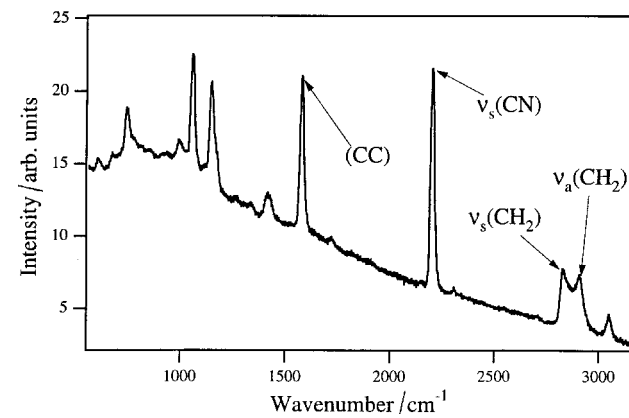

Figure 4. Raman spectrum of PCH5. The phenyl CC, ϕ(CC), and symmetric CN, ν_s(CN), stretches are used to monitor core motions and the symmetric, $\nu_s(CH_2)$, and anti-symmetric, $\nu_a(CH_2)$, methylene stretches are used to monitor the motions of the flexible pentyl group.

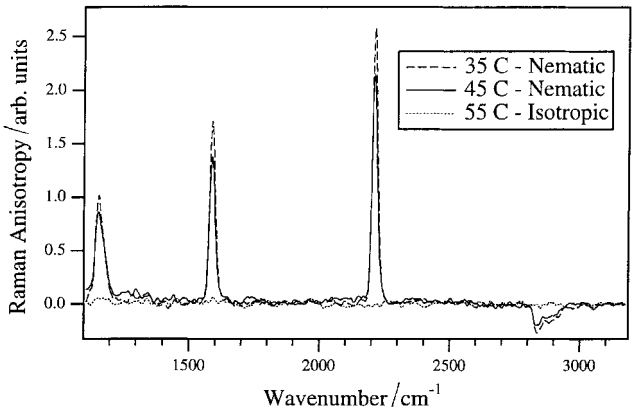

Figure 5. Raman anisotropy spectrum. Only orientation-sensitive peaks appear at temperatures in the nematic phase; no peaks appear in the isotropic phase.

Also, it is observed that the CH stretching bands exhibit a negative Raman anisotropy. The other large peak at 1177 cm^{-1} corresponds to the phenyl CH in-plane deformation. By positioning the monochromator to the wavenumbers of interest, the response of individual peaks to the applied electric field could be separately monitored.

Figure 6 shows an example of the response of the sample to a 4.5 V step at 35°C. The retardation and Raman anisotropy, normalized by the equilibrium value of R_{dc}, in response to the field that is turned on at 0 s and turned off at 20 s are shown. As expected, the magnitude of Γ decreases towards zero in the presence of the field and relaxes back to the quiescent state after the field is turned off. Due to the large refractive index anisotropy of these liquid crystals, the birefringence signal for the 125 μm sample goes through many orders of π as the director reorients. It is seen that Raman anisotropy provides a simpler measure of the reorientation since it is not incorporated within a trigonometric function.

From the response of the CN stretch, bulk orientational changes can be monitored. Figure 7 displays the saturation value of the Raman anisotropy from the CN bond as a function of the step voltage at 35°C. A threshold voltage of approximately 1.5 V is observed and is in agreement with that reported by Sugisawa *et al.* [28]. Also, the dependence of the rise time is calculated by exponentially fitting the CN response in the region after the induction region and is shown in figure 8. As predicted by equation (11), the inverse of the rise time is proportional to the square of the applied field.

Figure 9 shows the response of the CN band in the rise time region for various applied voltages at 35°C. This plot illustrates that there exists an induction period

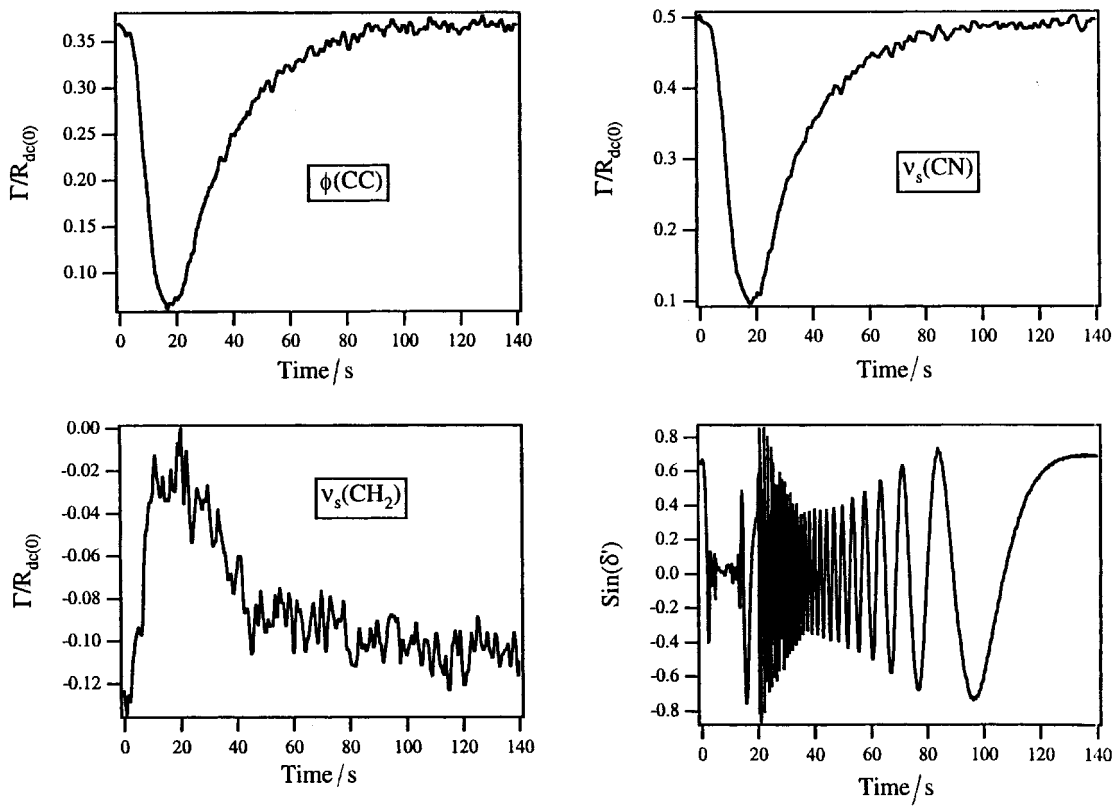

Figure 6. Raman anisotropy and birefringence signals in response to a 4.5 V step electric field at time = 0 s; the field is turned off at time = 20 s. Markers denote every 10th data point.

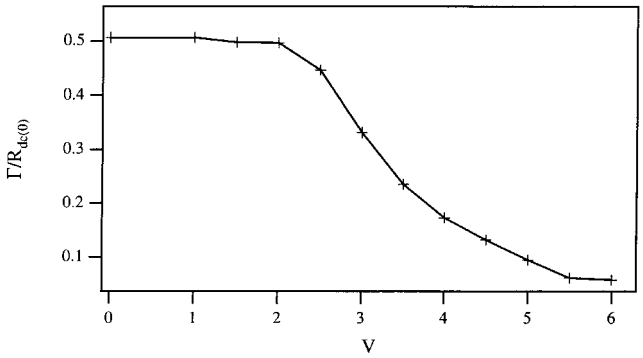

Figure 7. Steady state Raman anisotropy, normalized by the R_{dc} signal at zero field, vs voltage for the ν_s(CN) vibration.

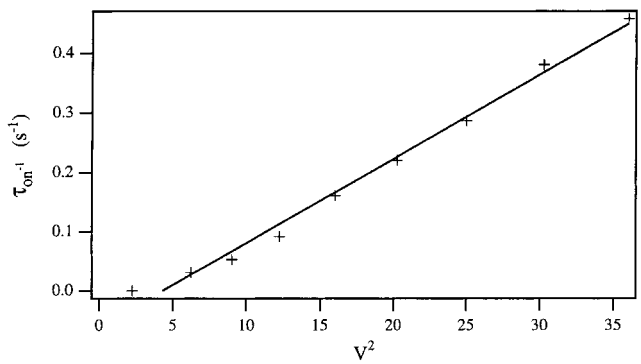

Figure 8. τ_{on}^{-1} vs voltage for the ν_s(CN) vibration.

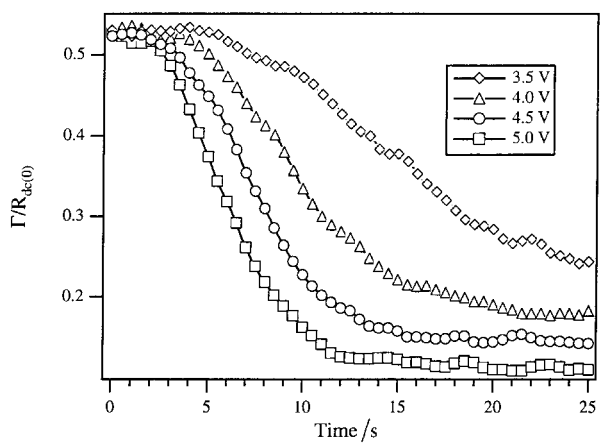

Figure 9. Response of Γ for the ν_s(CN) vibration within the rise time region. Markers denote every 10th data point.

before reorientation occurs. As described earlier, the initial stage of reorientation depends on director fluctuations to induce the transition from the metastable initial state to the stable state in the presence of the electric field. The director fluctuations at the onset of the field are, in turn, dependent on the magnitude of the applied field.

It is interesting to compare figure 9 with the birefringence signal which is a measure of the bulk response to the applied voltage. Figure 10 shows the

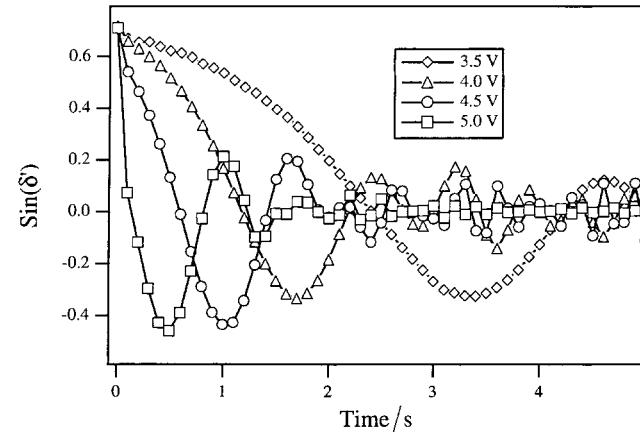

Figure 10. Birefringence signal for the first 5 s after the imposition of the step electric field. Markers denote every 10th data point.

birefringence signal at various voltages at short times after the field is turned on. Note that the non-ideal response displayed in figure 10 is commonly seen in liquid crystals [2] and polymer systems [29] where $\sin(\delta')$ is not smoothly varying between $+1$ and -1. This can be attributed to the fact that the birefringence lock-in amplifier is unable to respond as fast the the retardation passes through the multiple orders as a result of the Fréedericksz transition. This effect is most prominent after the field is turned on when the reorientation time is short in comparison with the relaxation time after the field is turned off. Also, the dispersive nature of the large retardation contributes to the non-ideal response. Figure 10, which plots only the first 5 s after the imposition of the field, as compared with figure 9 which plots the first 25 s, shows that the birefringence responds immediately to the applied field even though the CN bond experiences an induction period.

A comparison of the transient Raman anisotropy from bonds along the rigid core and flexible pentyl part provides insight into the differences in the micro-structural motions. Figure 11 displays the rise regime for the ϕ(CC), ν_s(CN), and $\nu_s(CH_2)$ stretches in response to a 5 V step at 0 s at 35°C. As described above, the CN bond exhibits an induction time. The ϕ(CC) vibration, which also probes the rigid core of PCH5, also displays an induction time. However, the Raman anisotropy from the CH stretch, which probes the flexible pentyl chain, responds immediately. The response of the $\nu_s(CH_2)$ vibration is similar to the response of the birefringence, as shown in figure 10, implying that short time response of the birefringence is mostly due to the reorientation of the pentyl chain. However, the fact that the motion of the flexible part precedes the reorientation of the rigid core is unexpected, since the electric torque on the

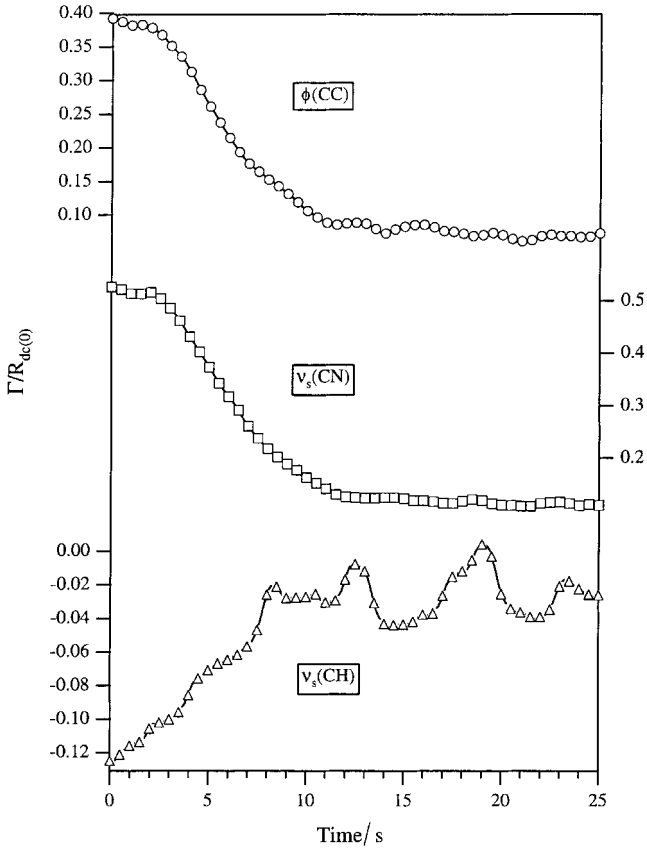

Figure 11. Response of the rigid core φ(CC) and ν_s(CN) vibrations and flexible pentyl group $\nu_s(CH_2)$ vibration to a 5 V step electric field. Markers denote every 10th data point.

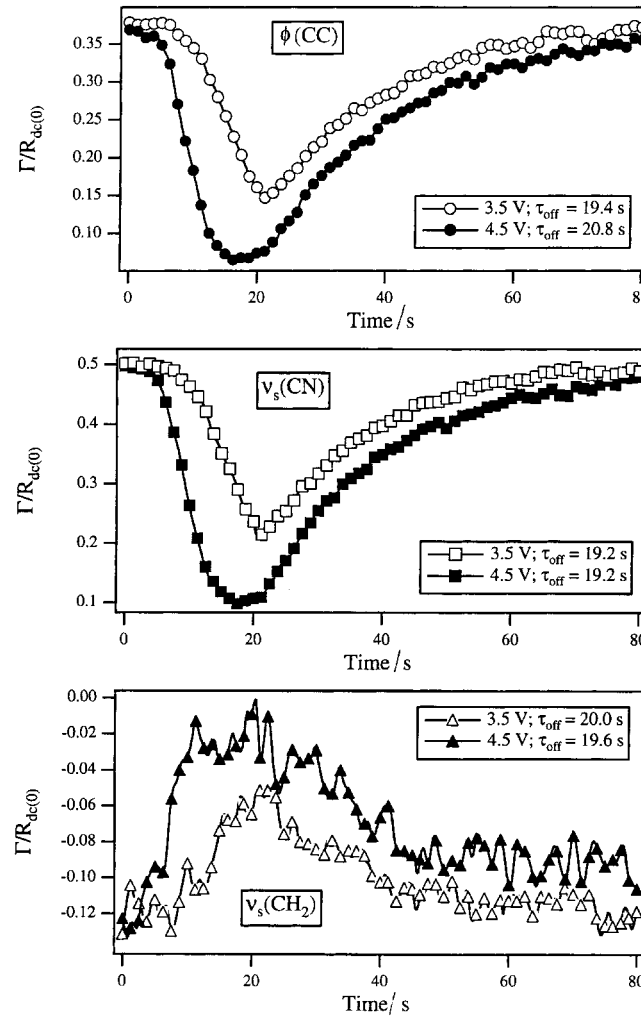

Figure 12. Raman anisotropy vs time in response to a 4.5 V electric field turned on at time = 0 s and off at time = 20 s. Markers denote every 10th data point.

molecules is believed to originate primarily from the dielectric anisotropy of the cyano and phenyl groups.

This peculiarity in the microstructural dynamics has been observed in 5CB using the polarized Raman microprobe technique of Booth *et al.* [30, 31] and time-resolved IR by Urano and Hamaguchi [5, 6]. Both groups observed that the reorientation of the flexible chain precedes the reorientation of the rigid core in response to the application of an electric field. However, Urano and Hamaguchi also observed a difference in the relaxation profiles of the bonds from the rigid and flexible parts after the field is turned off. Figure 12 displays the Raman anisotropy of the three bonds under investigation in response to an applied voltage of 4.5 V maintained from 0 to 20 s. This figure demonstrates that the relaxation time is the same for the entire molecule and is approximately 20 s, independent of the applied voltage. The value for the relaxation time is in good agreement with the value of 18 s calculated from equation (12) using values of $\gamma_r = 110$ cp and $K_{11} = 9.6$ pN (data obtained from EM Industries for PCH5 in the supercooled nematic state at 20°C). Urano and Hamaguchi report an inertial effect where, even after the field is switched off, the rigid core of 5CB continues to orient while the alkyl part immediately relaxes back to the no-field orientation [5]. However, it is possible that the difference in relaxation is a result of back flow, since Urano and Hamaguchi apply voltage pulses greater than 10 V to study the response of 5CB, which has a threshold voltage of 1.5 V [32]. It has been reported that, for voltages greater than 4 times the threshold voltage, back flow can cause non-monotonic relaxation of the director after the field is switched off [2]. The presence of a flow would tend to affect the rigid core more than the flexible part. The observation that the rigid and flexible parts reorient differently in response to the step voltage, but relax identically after the voltage is removed, indicates that there is a mechanism by which the electric field couples with the alkyl portion of the molecule.

In order to gain a better understanding of the microstructural dynamics within PCH5, the Raman anisotropy from the various bonds was monitored in response to a sinusoidally varying electric field. Before acquiring data, the sample was subjected to many cycles of the oscillatory field until a steady state was achieved. The Raman anisotropies arising from the different vibrational modes were Fourier transformed to obtain the amplitude and phase with respect to the applied voltage. These values allow for cross correlation of the response from distinct bond groups using equations (6) and (7).

Figure 13 shows the cross correlation of the Raman anisotropy emanating from different wavelengths. The synchronous and asynchronous responses are typically shown in the form of a contour plot; however, since this study is concerned with the motions of only two sections of the molecule, the rigid core and flexible part, figure 13 displays the one dimensional cross correlation functions with respect to the CN stretch for easier interpretation. The synchronous plot shows that the CN bond reorients in a highly cooperative manner with the other liquid crystal bond groups. This is not surprising since the bond vibrations originate from within the same molecule. The asynchronous plot provides more interesting results. $\Psi(2226\,\mathrm{cm}^{-1}, \nu)$ shows that the only resolvable feature is the asynchronous correlation of the CH profile with the CN peak. Thus, as seen in the step electric field experiments, the rigid core and flexible part exhibit different time-dependent responses. In fact, the non-cooperative motions increase the resolution within the CH profile such that the methylene symmetric stretch ($2857\,\mathrm{cm}^{-1}$), methyl symmetric stretch ($2870\,\mathrm{cm}^{-1}$), and the methylene anti-symmetric stretch ($2926\,\mathrm{cm}^{-1}$) can be separately identified. Also it is interesting to note that the magnitude of the asynchronous correlation between the CN and CH bands is of the same order as the synchronous intensity.

In order to identify the variation of the submolecular motions between the two parts of the molecule, a frequency sweep was performed for the wavelengths of interest. Figure 14 displays the amplitude of the Raman anisotropy in response to a 5 V amplitude oscillatory field. At periodities that are much longer than the bulk reorientation times, the PCH5 molecules orient easily with the field and, therefore, exhibit large amplitude responses. The response for both the rigid core and flexible alkyl group decreases as the frequency increases. Ultimately, at high frequencies, the rigid core is unable to reorient with the electric field and its motion is inhibited. However, beyond this point figure 14 shows that the amplitude of the pentyl group is actually enhanced until it also is immobilized at even higher frequency. Thus, the alkyl chain can reorient in the presence of an electric field independently of the rigid core. This observation is complementary to the step electric field data since short times after the step correspond to high frequencies.

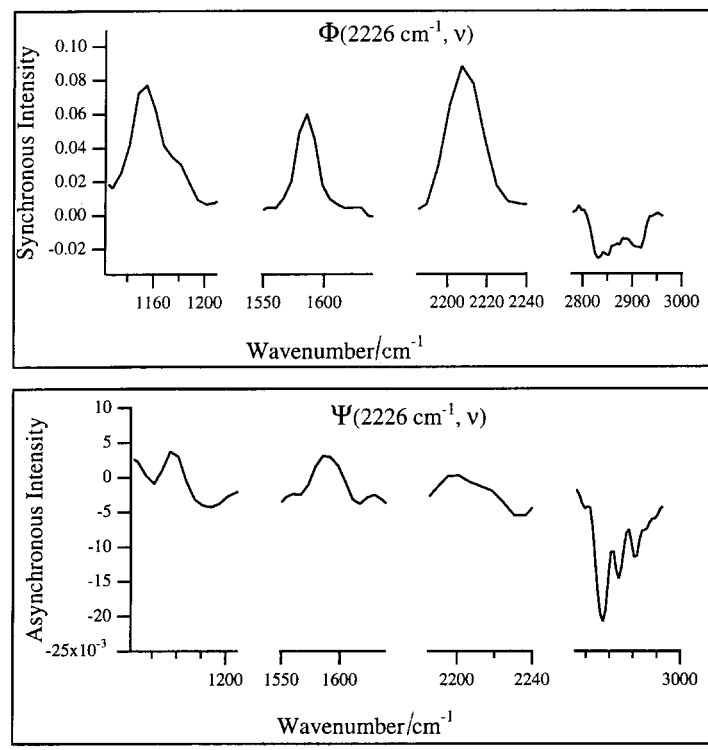

Figure 13. Synchronous and asynchronous intensity with respect to $\nu_s(\mathrm{CN}) = 2226\,\mathrm{cm}^{-1}$ for PCH5 subjected to a sinusoidal voltage of 5 V amplitude at 0.01 Hz at 35°C.

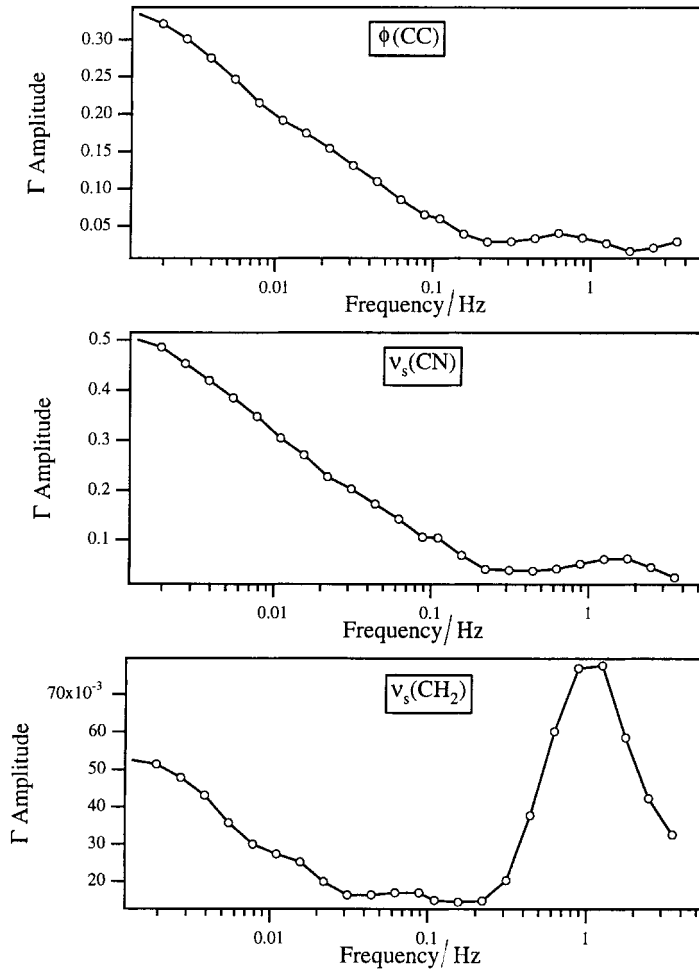

Figure 14. Raman anisotropy amplitude vs frequency in response to a 5 V amplitude sinusoidal electric field.

Both the oscillatory and step data suggest a mechanism for the electric field-induced reorientation of PCH5 and similar liquid crystals. There appears to be a local dielectric anisotropy associated with the alkyl chain that causes a torque in the presence of an electric field. The torque results in an independent reorientation of the pentyl chain by an internal rotation of the C(pentyl)–C(cyclohexane) bond. The observation that both the rigid core and flexible group relax identically when the field is turned off implies that the liquid crystal molecules reorient as rigid rods in the absence of a field. However, in the presence of an electric field, it is seen that the pentyl group can reorient before the rigid core immediately after the field is turned on. Also, unlike the rigid core, the flexible group does not exhibit an induction period. Based upon the proposed mechanism, the lack of an induction time indicates that the pentyl chain is not initially oriented in the metastable state perpendicular to the electric field. This is in agreement with the NMR results of Fung *et al.* [33] which show that the rigid core has significantly higher order parameters than the pentyl chain of 5CB. Also, Kaito *et al.* [34] used isomeric state theory to calculate an angle of 52° between the long axis of the cyanobiphenyl core and the long axis of the pentyl chain.

The high frequency observation that the flexible part reorients while motion of the rigid core is inhibited also supports the existence of a local dielectric anisotropy for the flexible tail. This local dielectric anisotropy, which is small compared with that associated with the rigid core, allows for a collective reorientation of the flexible tails within the sample when the motion of the rigid parts is restricted. This mechanism of pentyl group reorientation due to a coupling with the electric field is fundamentally different from the mechanism proposed by Urano and Hamaguchi [7]. These authors propose that perturbed surface molecules induce the internal rotation of the C(pentyl)–C(biphenyl) bond within the bulk for 5CB. However, the results from this work show that high frequencies hinder the reorientation of the rigid part of the molecules within the bulk. The surface molecules would most likely be impeded before the bulk

molecules due to the presence of the wall, but at these frequencies it is seen that the motions of the pentyl group are actually amplified.

5. Conclusions

Two-dimensional Raman scattering has been introduced as a technique to study submolecular dynamics in liquid crystals. In order to demonstrate the potential of 2D Raman, the liquid crystal PCH5 has been investigated. The motions of both the rigid core and flexible tail were monitored in response to step and oscillatory electric fields. The experiments show that for short times after the step and for high oscillatory frequencies, the pentyl groups collectively reorient independently of the rigid core.

Based on these observations, a molecular mechanism for the electric field-induced reorientation is proposed. The data suggest the existence of a local dielectric anisotropy associated with the pentyl chain. For short times after the imposition of an electric field, the flexible group reorients by an internal rotation of the C(pentyl)–C(cyclohexane) bond. Since this process occurs on time scales that are much longer than those associated with internal molecular motions, it is obviously a collective process over the sample thickness. After the induction period for the rigid core, the PCH5 molecule reorients cooperatively. Unlike the mechanism proposed by Urano and Hamaguchi [6], the reorientation of surface molecules is not an important contribution to the reorientation of the bulk.

Our observations also indicate the existence of multiple reorientation times within liquid crystals. Similar observations of asynchronous intramolecular motions between the main chain and side groups of polymers subjected to mechanical perturbations have been reported, faster than characteristic relaxation times, above the glass transition temperature [4] and approaching the mechanical glass transition [4]. As with the study of polymer dynamics, frequency sweep experiments are useful in probing cooperative reorientation within liquid crystals over many time scales. Additionally, compared with IR spectroscopy, Raman scattering offers the advantage of studying thicker samples that have longer electric field-induced reorientation times and are less influenced by surface molecules.

The financial support of Eastman Kodak is gratefully acknowledged.

References

[1] Blinov, L. M., 1983, *Electro-optical and Magneto-optical Properties of Liquid Crystals* (New York; John Wiley and Sons).

[2] Blinov, L. M., and Chigrinov, V. G., 1994, *Electrooptic Effects in Liquid Crystal Materials* (New York: Springer-Verlag).

[3] Houssier, C., and Fredericq, E., 1973, *Electric Birefringence and Electric Dichroism* (London: Oxford University Press).

[4] Huang, K., Archer, L. A., and Fuller, G. G., 1996, *Macromolecules*, **29,** 966.

[5] Urano, T. I., and Hamaguchi, H., 1992, *Chem. Phys. Lett.*, **195,** 287.

[6] Urano, T. I., and Hamaguchi, H., 1993, *Appl. Spectrosc.*, **47,** 2108.

[7] Shilov, S. V., Okretic, S., and Siesler, H. W., 1995, *Vib. Spectrosc.*, **9,** 57.

[8] Katayama, N., Sato, T., Ozaki, Y., Murashiro, K., Kikuchi, M., Saito, S., Demus, D., Yuzawa, T., and Hamaguchi, H., 1995, *Appl. Spectrosc.*, **49,** 977.

[9] Czarnecki, M. A., Okretic, S., and Siesler, H. W., 1997, *J. phys. Chem. B*, **101,** 372.

[10] Katayama, N., Czarnecki, M. A., Satoh, M., Watanabe, T., and Ozaki, Y., 1997, *Appl. Spectrosc.*, **51,** 487.

[11] De Bleijser, J., Leyte-Zuiderweg, L. H., Leyte, J. C., van Woerkom, P. C. M., and Picken, S. J., 1996, *Appl. Spectrosc.*, **50,** 167.

[12] Archer, L. A., Huang, K., and Fuller, G. G., 1994, *J. Rheol.*, **38,** 1101.

[13] Noda, I., 1989, *J. Amer. chem. Soc.*, **111,** 8116.

[14] Noda, I., 1990, *Appl. Spectrosc.*, **44,** 550.

[15] Noda, I., 1993, *Appl. Spectrosc.*, **47,** 1329.

[16] Freedericksz, V., and Zolina, V., 1933, *Trans. Faraday Soc.*, **29,** 919.

[17] Dueling, H., 1972, *Mol. Cryst. liq. Cryst.*, **19,** 123.

[18] Gruler, H., and Meier, G., 1972, *Mol. Cryst. liq. Cryst.*, **16,** 299.

[19] Pieranski, P., Brochard, F., and Guyon, E. H., 1972, *J. de Phys.*, **33,** 681.

[20] Helfrich, W., 1973, *Mol. Cryst. liq. Cryst.*, **21,** 187.

[21] Pieranski, P., Brochard, F., and Guyon, E. H., 1973, *J. de Phys.*, **34,** 35.

[22] Brochard, F., 1973, *Mol. Cryst. liq. Cryst.*, **23,** 51.

[23] Clark, M. G., and Leslie, F. M., 1978, *Proc. roy. Soc. London*, **A361,** 463.

[24] Archer, L. A., Fuller, G. G., and Nunnelley, L., 1992, *Polymer*, **33,** 3574.

[25] Horowitz, P., and Hill, W., 1989, *The Art of Electronics* (New York: Cambridge University Press).

[26] Seeliger, R., Haspelko, H., and Noack, F., 1983, *Mol. Phys.*, **49,** 1039.

[27] Gray, G. W., and Mosley, A., 1976, *Mol. Cryst. liq. Cryst.*, **35,** 71.

[28] Sugisawa, H., Toriumi, H., and Watanabe, H., 1992, *Mol. Cryst. liq. Cryst.*, **214,** 11.

[29] Fuller, G. G., 1995, *Optical Rheometry of Complex Fluids* (New York: Oxford University Press).

[30] Booth, K. M., Nash, J., and Coles, H. J., 1992, *Meas. Sci. Tech.*, **3,** 843.

[31] Booth, K. M., and Coles, H. J., 1993, *Liq. Cryst.*, **13,** 677.

[32] Toriumi, H., Sugisawa, H., and Watanabe, H., 1988, *Jpn. J. appl. Phys.*, **27,** L935.

[33] Fung, B. M., Afzal, J., Foss, T. L., and Chau, M., 1986, *J. chem. Phys.*, **85,** 4808.

[34] Kaito, A., Wang, Y. K., and Hsu, S. L., 1986, *Anal. Chim. Acta*, **189,** 27.